Biochemical and Biophysical Research Communications 452 (2014) 408–414

Contents lists available at ScienceDirect

Biochemical and Biophysical Research Communications

journal homepage: www.elsevier.com/locate/ybbrc

Structural insights into the interaction of blood coagulation co-factor VIIIa with factor IXa: A computational protein–protein docking and molecular dynamics refinement study

Divi Venkateswarlu *

Department of Chemistry, North Carolina Agricultural and Technical State University, Greensboro, NC 27411, USA

ARTICLE INFO

Article history:
Received 9 August 2014
Available online 23 August 2014

Keywords:
Factor VIIIa
Factor IXa
Blood clotting
Protein–protein docking
Molecular dynamics
Tenase complex

ABSTRACT

Coagulation factor X (FX) zymogen activation by factor IXa (FIXa) enzyme plays a critical role in the middle-phase of coagulation cascade. The activation process is catalytically inert and requires FIXa binding and complex formation with co-factor VIIIa (FVIIIa). In order to understand the structural details of the FVIIIa:FIXa complex, we employed knowledge-driven protein–protein docking and aqueous-phase MD refinement methods to develop a stable structural complex between FVIIIa and FIXa. The model shows that all four domains of FIXa wrap across FVIIIa that spans the co-factor binding surface of A2, A3 and C1 domains. The region surrounding the 558-helix of the A2-domain of FVIIIa is predicted to be the key interaction site with the helical segments of Lys293–Lys301 and Asp332–Arg338 residues of the serine-protease domain of FIXa. The hydrophobic helical stack between the GLA and EGF1 domains of FIXa is predicted to be primary interacting region with the A3–C2 domain interface of FVIIIa.

1. Introduction

Intrinsic pathway of blood coagulation involves the proteolytic activation of zymogenic factor X (FX) by serine protease IXa (FIXa) in the presence of anionic membrane phospholipid (PL) surface and divalent metal ions. This reaction is catalytically inert and requires critical binding of the co-factor VIIIa (FVIIIa) with FIXa [1]. FVIIIa increases the catalytic rate constant (K_{cat}) of FX activation by FIXa several orders ($\sim 10^6$-fold) of magnitude. The role of FVIIIa is to reduce the K_d for its interaction with FIXa and the K_m for substrate FX [2]. FVIIIa circulates in blood as a hetero-trimer among A1, A2 and contiguous A3–C1–C2 subunits. Factors IX and X are homologous vitamin-K dependent (VKD) membrane binding serine proteases with each being characterized by four domains: GLA, EGF1, EGF2 and SP. Factor IXa enzyme is composed of two chains covalently linked by a disulfide bond between the 145 residue length light chain (composed of GLA, EGF1 and EGF2) and the 235 residue length heavy chain (composed of SP domain) [3]. The enzyme activity of FIXa is centered in the serine-protease (SP) domain that features the catalytic triad residues: His221, Asp269, and Ser365 [4]. Factor X is a 448 residue length zymogenic precursor to functionally active FXa with similar domain organization of FIXa with a 55-residue length activation peptide (AP) located between EGF2 and SP domains [5].

Activation of FX by FIXa:FVIIIa complex, known as the intrinsic tenase complex, results in the loss of 55-residue activation peptide and subsequent formation of activated FX (FXa). The functional importance of FVIIIa–FIXa tenase complex and its role in FX activation is illustrated by hemophilia in which the absence of either protein causes life-threatening bleeding disorders. Similarly, genetic mutations in FIXa are associated with the bleeding diatheses hemophilia B. In contrast, high levels of FVIII activity have recently been reported to be associated with an increased risk of thrombosis. Due to the therapeutic importance of FVIIIa/FIXa complex and its role in FX activation, a number of experimental and structural studies have been directed towards understanding the structure–function relationship among the three proteins [6,7]. Despite the great progress in biochemical characterization of specific inter- and intra-protein binding sites between FVIIIa and FIXa in the Xase complex, the accurate atomistic details of molecular recognition mechanism of FX activation are largely unclear primarily due to lack of high-resolution X-ray crystal structures for complete models of FVIIIa, FIXa and the FVIIIa:FIXa complex.

We present our modeling efforts in developing the solution structure for the tenase complex between FVIIIa and FIXa, based on the solvent-equilibrated structures of FVIIIa and FIXa, by employing a systematic grid-based protein–protein docking approach, guided by a large body of experimental data. The docked

* Fax: +1 336 334 7124.
E-mail address: divi@ncat.edu

http://dx.doi.org/10.1016/j.bbrc.2014.08.078
0006-291X/

complex was subsequently refined by explicit-solvent molecular dynamics (MD) simulations. The proposed model of the complex identifies critical enzyme-cofactor interaction sites that are consistent with the experimental findings.

2. Materials and methods

2.1. Modeling the structure of factor VIIIa

FVIIIa is a non-covalently bound hetero-trimer of 1383 residues among the A1 (Ala1–Arg372), A2 (Ser373–Arg740), A3–C1–C2 (Ser1690–Tyr2332) domains. Based on an incomplete medium resolution (3.8 Å) X-ray crystal structure of FVIII (PDB ID: 3CDZ), the full length solution structure of B-domain less FVIII was published previously from our laboratory [8]. Starting from the solution structure of FVIII zymogen, extracted from the 100 ns of MD trajectory, the active form of FVIII was generated with explicit cleavages at Arg372, Arg740 and Arg1690 residues, creating a hetero-trimer among A1, A2 and A3–C1–C2 domains. The resulting structure was subjected to 200 ns of MD refinement in explicit water based on the simulation protocol outlined in the Supplemental data.

2.2. Modeling of the full-length FIXa enzyme structure

The activated factor IX is a four domain VKD serine-protease with four contiguous domains of GLA, EGF1, EGF2 and SP domains. The characteristic Ca^{+2}-bound ω-loop at the N-terminus of the GLA domain is widely known to insert into the PL surface. The GLA domain aligns vertically on the platelet surface with the SP domain located at ~85 Å distance remote from the membrane surface (shown in Fig. 1 together with FVIIIa and FX zymogen structures). The EGF1 and EGF2 domains serve as the spacer domains between GLA and SP domains. While there is no full length X-ray crystal structure for human form of FIXa enzyme, a number of X-ray/NMR structures have been reported for partial structures of EGF2-SP, EGF1 and GLA domains [9,10]. Also, a medium resolution (3.0 Å) crystal structure for full length porcine FIXa (PDB ID: 1PFX) was published [11]. We constructed the full structure of FIXa (human) by optimally aligning the backbone atoms of the X-ray crystal structures of the human forms of EGF2-SP (PDB ID: 3KCG; 1.7 Å), EGF1 (PDB: 1EDM; 1.5 Å) and GLA (PDB: 1J35; 1.8 Å) domains with the structural template of full model of porcine FIXa. The conformations of linking regions between the three segments were adjusted by loop refinement using MODLOOP program within CHIMERA software [12].

3. Results and discussion

3.1. Solution structure of FVIIIa co-factor

The structure of FVIIIa, derived from solution structure of FVIII as described in Section 2.1, was subjected to 200 ns of MD refinement in explicit water. Full convergence of the structure was achieved over the first 100 ns of simulation as shown by the RMS deviations from the starting conformation (Fig. 2A). In the original X-ray structure (PDB ID: 3CDZ), from which FVIII model was derived, several solvent-exposed regions were not well-resolved or completely missing [13]. One of these regions corresponds to functionally important loop region (Tyr555–Arg571) of the A2 domain. In the two reported crystal structures (2R7E and 3CDZ), this loop was predicted to have conflicting conformations. Over the simulation period, we noticed that the loop region folded into a helical conformation as shown in Fig. S1. We generated five representative solution structures of FVIIIa by clustering the last 100 ns of the MD trajectory. The backbone superimposed structures of the models are presented in Fig. S2A. Since the focus of the current study is to model the FVIIIa.FIXa complex, we defer from detailed discussion about the structure of FVIIIa that was already described in our previous work [8].

3.2. Solution structure of FIXa enzyme

The structural model of FIXa, comprised of the light-chain (Tyr1–Lys142) and the heavy-chain (Val181–Thr415), was

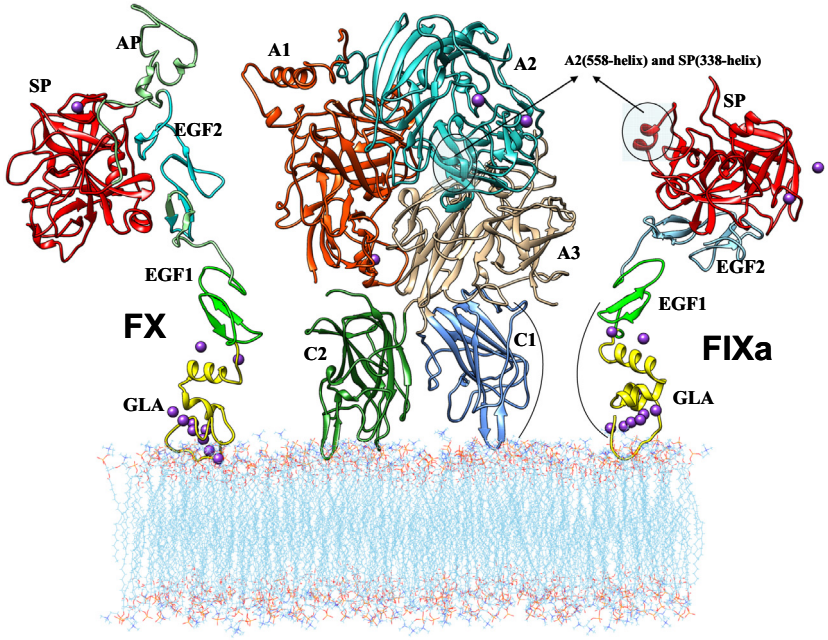

Fig. 1. Alignment of the full models of FVIIIa cofactor (center), FIXa enzyme (right) and FX zymogen (left) on the hypothetical phospholipids membrane surface. The membrane surface is for only illustrative purpose and not explicitly modeled in the current study. The functionally relevant interacting regions between FVIIIa and FIXa are highlighted.

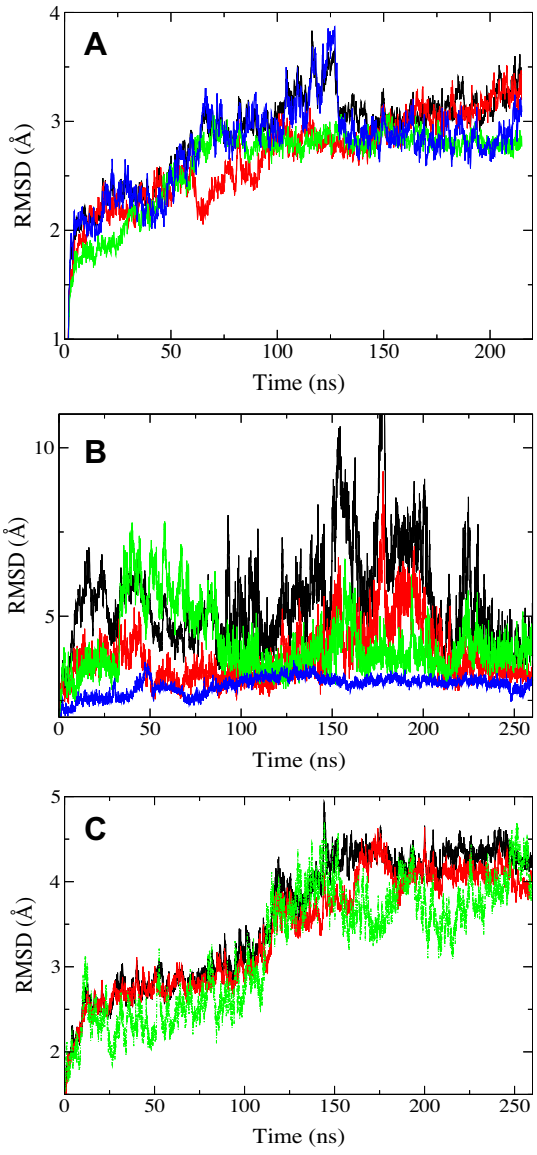

Fig. 2. (A) RMS deviations in FIXa simulation with plots of fluctuations in GLA-EGF1 (red), EGF1-EGF2 (green), EGF2-SP (blue) and all domains together (black); (B) RMS deviations in FVIIIa simulation with plots of fluctuations in A1 (red), A2 (green), A3–C1–C2 (blue) and all five domains together (black); (C) RMS deviations in FVIIIa:FIXa complex with plots of fluctuations in FVIIIa (black), FIXa (red) and FVIIIa;FIXa complex (green). (For interpretation of the references to color in this figure legend, the reader is referred to the web version of this article.)

simulated for 250 ns in explicit water. The RMS deviations over the simulation period for GLA-EGF1, EGF1-EGF2 and EGF2-SP domains are shown in Fig. 2B. It is evident from the plot that FIXa exhibits high-degree of flexibility at the interface of GLA-EGF1 and EGF1-EGF2 domains. The flexibility is largely attributed due to weak domain–domain interactions. The interface between the EGF2 and SP domains is mostly rigid due to the presence of disulfide bond between the two domains and relatively strong stabilizing forces. It is evident from the plot that the EGF2-SP domains are well stabilized (blue color) with overall RMSD of ~1.5 Å from the starting structure while the GLA-EGF1 and EGF1-EGF2 domains showed significant flexibility.

The membrane-binding GLA domain residues Leu6 and Phe9 residues are believed to immerse into the anionic phospholipids surface with the catalytic protease domain positioned vertically far from the membrane surface (Fig. 1). It is estimated from the recent FRET experimental studies that the distance from the catalytic triad residue Ser365 to the membrane surface as ~85 Å [14]. In order to assess this distance over the simulation period, we computed the backbone Cα–Cα atoms distance between Ser365 of the SP domain and Leu6/Phe9 residues of the GLA domain. The measured distance varies widely from 70 Å to 100 Å over the simulation time. Such large fluctuations could be attributed due to the inherently weak inter-domain interactions among GLA, EGF1 and EGF2 domains. In order to generate the optimal structure of FIXa for the proposed docking studies with FVIIIa in the current study, we generated a conformational ensemble of 30 structures based on clustering the MD trajectories over the last 50 ns of simulation time. To be consistent with the experimental FRET data, we selected five structures from the pool of clusters where the distance between the Ser195 of catalytic domain and the Leu6/Phe9 of GLA domain is ~85 ± 5 Å. The backbone superimposed structures of five models are shown in Fig. S2B. These structures were subsequently used for molecular docking with FVIIIa.

3.3. Modeling the tenase complex between FVIIIa and FIXa

In the absence of experimental structure for the tenase complex, we employed the protein–protein docking methods to obtain the putative FVIIIa:FIXa complex. The application of grid-based docking methodology is often successful for proteins whose crystal structures have been well resolved and *a priori* knowledge of likely interaction sites between the two docking partners is readily available for post-processing of the docked complexes [15]. Protein–protein docking methods produce hundreds of possible complexes and the most daunting task is to identify the near-native complex among the pool of possible binding poses [16]. Typically for blind docking studies, such as in our present study where the precise nature of how FVIIIa binds to FIXa enzyme is unknown, a set of known residue/domain level interactions between the two proteins often guide narrowing the likely complexes to possibly ten or less for further analysis.

A number of site-specific mutagenesis and domain-swapping studies have been reported in order to understand the functional role of various domains of FVIIIa and FIXa involved in the tenase complex formation [7,17,18]. The A2 and A3 domains have been largely implicated to possess the binding interface with SP and EGF domains of FIXa respectively. The GLA domain of FIXa was implicated to interact with the light-chain of FVIIIa, though it was not clear whether the interaction is with C1 or C2 domains or both [19]. However, the projection of full models of FVIIIa and FIXa on PL surface (Fig. 1) provides a structural rationale that the C1 domain is most likely the interacting region with GLA domain. While there were some suggestions, based on peptide inhibition studies, that the C2 domain of FVIIIa might possess interaction sites for FIXa light-chain, our initial attempts to generate a docking model with simultaneous interactions of SP and GLA domains of FIXa with A2 and C2 domains of FVIIIa respectively did not result in meaningful models.

Guided by the large body of published experimental studies and existing hypothesis of platelet initiated clotting pathways, we developed the following criteria in narrowing the possible docked solutions to the putative structural complex. The most plausible structural complex between FVIIIa and FIXa must satisfy the criteria of distance/spatial constraints (see Fig. 1. for alignment of FVIIIa and FIXa on hypothetical membrane surface) such that

(i) The GLA domain of FIXa and C1–C2 domains of FVIIIa must align at the same plane on the anionic phospholipid surface.
(ii) The Tyr555–Arg571 (558-helix) segment of the A2-domain of FVIIIa must be in contact distance with Asp332–Arg338 (338-helix) helical region of the SP domain of FIXa.

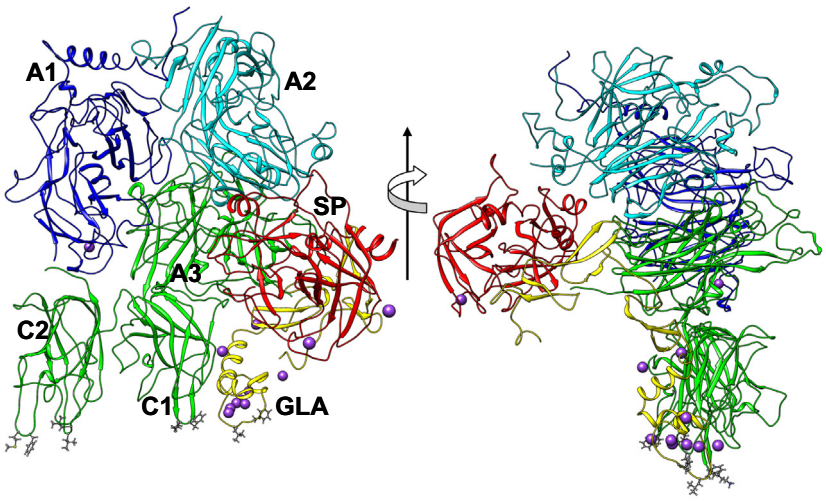

Fig. 3. The solution structure of the FVIIIa:FIXa tenase complex based on the MD snapshot extracted from 250 ns of simulation trajectory.

(iii) The putative tenase complex should be able to explain the surface mutations in the loop regions of A2, A3 and C1 domains that could possibly be involved in FIXa interactions, as reported by patient mutational data in Hemophilia-A database.

(iv) The active-site region of FIXa, located in the SP domain, must be sufficiently solvent-exposed and aligned in proper orientation such that the tenase complex facilitates productive docking of the 55-residue length activation peptide of the incoming FX zymogen.

By incorporating the above criteria, we performed docking calculations on four solution structures of FVIIIa and FIXa extracted from the converged MD trajectories of the simulations (shown in Fig. S2). While there are several docking algorithms exist in literature that follow the shape-based grid docking approach to generate protein–protein complexes, we chose PATCHDOCK program due to its ability to narrow the docked complexes using distance-based filtering criteria [19,20]. It should be mentioned that our goal of using the grid-based docking approach was only to generate an approximate initial structural complex between the two proteins that satisfy most of the above-mentioned criteria. No critical analysis of the binding surfaces of the docked complexes was attempted due to non-physical nature of the shape-based grid surfaces, generated during docking, since further refinement by all-atom MD simulations is expected to dynamically relax the bind surfaces over the simulation period. We performed four docking calculations with the clustered structures of FVIIIa and FIXa in order to allow conformational variability of the solution structures. By narrowing the docked solutions from the four docking experiments based on the above-mentioned filtering criteria, a consensus structural complex between the two proteins was selected among ~150 possible docked solutions.

3.4. Global features of the FVIIIa:FIXa tenase complex

The docked complex of FVIIIa:FIXa was subjected to MD refinement for 260 ns in explicit water. The analysis of RMS deviation over the simulation trajectory shows that the complex is well-stabilized though the binding surface between the two proteins shows some degree of flexibility (Fig 2C). It may be observed from the plot that while the RMS fluctuations in FVIII and FIXa were relatively small, the fluctuations appear much wider when both proteins in the complex are considered. This illustrates the dynamic nature of the protein–protein interactions between the two proteins. The equilibrated structure of FVIIIa.FIXa complex (snapshot from 260 ns) is shown in Fig. 3 in two orientations. In

Table 1
Hydrogen bonding interactions between the FVIIIa and FIXa domains within the tenase complex.

Donor/acceptor	Residues	%Pop	Distance	Angle
FIXa(LC):FVIIIa interactions				
Gla36 (OE1)	***Lys2136(NZ)***	***34***	***2.77***	***86.7***
Asn67(O)	Thr1739(OG1)	59	2.79	159.5
Asn67(OD1)	Gln1745(NE2)	47	2.84	49.5
Asn67(ND2)	Pro1746(O)	66	2.85	156.2
Asn67(ND2)	Tyr1748(H)	52	2.69	89.4
Asn67(ND2)	Leu1747(HA)	29	2.83	92.4
Asn67(ND2)	Tyr1748(H)	52	2.69	90.0
Ser68(OG)	Thr1739(HB)	42	2.68	66.7
Glu78(OE1)	His1697(NE2)	46	2.83	154.3
Glu78(OE2)	Thr1695(OG1)	38	2.70	162.8
Lys80(NZ)	Thr1739(O)	63	2.81	80.79
Thr87(OG1)	Gln1798(OE1)	50	2.77	159.5
Thr87(OG1)	Phe1816(HE2)	42	2.77	87.7
Asn89(ND2)	Gln1798(OE1)	32	2.85	82.2
Asn89(O)	Lys1818(NZ)	79	2.82	86.5
Lys91(HG3)	Thr1695(OG1)	31	2.69	83.43
Lys91(N)	Asn1770(OD1)	60	2.87	159.7
Lys91(NZ)	Lys1693(O)	53	2.82	83.9
Arg94(HH21)	Thr1695(OG1)	21	2.70	114.1
Asp104(OD1)	***Arg1797(NH2)***	***75***	***2.81***	***159.1***
Asn101(ND2)	Arg1797(O)	26	2.86	60.6
FIXa(SP):FVIIIa interactions				
Asn258(ND2)	Arg740(HA)	26	2.78	110.9
Asn267(ND2)	PRO739(O)	70	2.86	49.9
Asn267(ND2)	Glu738(OE2)	51	2.83	165.9
Lys301(HE2)	Gln1820(NE2)	22	2.75	56.9
Lys301(NZ)	***Glu683(OE1)***	***42***	***2.81***	***89.7***
Tyr306(OH)	Phe1691(HB2)	27	2.79	94.3
Arg327(NH2)	***Glu1768(OE1)***	***54***	***2.79***	***160.7***
Arg333(NH2)	Met567(HG2)	28	2.74	72.8
Thr340(O)	Arg562(NH1)	78	2.82	50.1
Phe341(O)	Arg562(NH1)	76	2.84	57.9
Thr343(OG1)	Arg562(HG2)	70	2.71	63.7
Asn346(N)	Ile566(HA)	85	2.71	77.3
Asn346(N)	Gln565(O)	42	2.89	131.4
His354(NE2)	Lys1827(HB2)	30	2.82	63.2
Glu372(OE2)	Gln1692(NE2)	80	2.81	163.7
Glu372(OE2)	Phe1691(N)	43	2.85	153.7
Glu372(OE1)	Ser1690(N)	40	2.83	84.5
Gly375(HA2)	Ser1690(OG)	36	2.74	60.5
Gly375(H)	Gln1692(NE2)	34	2.66	86.6
Arg403(NH1)	***Glu738(OE1)***	***60***	***2.85***	***49.9***

The ion-pair interactions are highlighted.

order to assess the buried surface area (BSA) between the two proteins, we estimated the average solvent-accessible surface area (SASA), based on 10 solution structures extracted over the last 20 ns of MD trajectory, using NACCESS program [21]. Based on the default probe radius of 1.4 Å, we estimated the total BSA between the two proteins as 4466 Å^2 out of which 59% (2619 Å^2) of the surface is non-polar and 41% (1847 Å^2) is polar. This suggests that the interface is composed of more non-polar interactions. Calculation of the binding free-energy between the two proteins in the complex by MM-PBSA method (based on 500 frames extracted from last 20 ns of MD trajectory) estimates that the complex is stabilized by $\Delta\Delta G_{BIND}$ of ~100 kcal/mol with the contribution of gas-phase energy of −2130 kcal/mol and the solvation energy of 2230 kcal/mol. Based on the last 50 ns of the MD trajectory, we computed the hydrogen-bonding interactions between the two proteins and are tabulated in Table 1.

3.5. A2 domain interactions with EGF2-SP domains

The equilibrated structural complex shows that the 558-helix of the A2 domain binds to the common surface generated by the 300-helix and 338-helix of the SP domain of FVIIIa (Fig. 4A). The region surrounding the 558-helix, spanning Tyr555–Arg571 residues, has been implicated in several experimental studies as an important FIXa binding region [7,18]. In the proposed model, the 338-helix (Asp332–Arg338) of the SP domain of FIXa interacts with a deep cleft pocket created by the exposed surface region between the A2 and A3 domains. The possible hydrogen-bonding interactions between the two proteins are listed in Table 1. The 558-helix residues (Arg562, Gln565, Ile566 and Met567) of the A2 domain form stable H-bonding interactions with 338-helix in the SP domain of FIXa. The mutation of Gln565 to Lys, Arg or His was implicated to cause moderate to severe hemophilia-A in patients. In the complex, the side-chain of Gln565 interacts with the side-chain of Lys265 via H-bond and van der Waals' interactions with the side-chain of Tyr345 of the FIXa. Mutation of Gln565 to positive-charged Lys or Arg can be expected to cause significant charge-repulsion and might lead to destabilization of the complex formation. Similarly, the side-chain of Ile566 forms hydrophobic interactions with Ile344 of the SP domain. The Thr mutation at Ile566 was implicated to cause severe hemophilia. The Ile → Thr mutation might cause some degree of charge repulsion and perhaps trigger conformational changes in the 558-helical region, causing altered binding interactions between the two proteins.

In addition to the 338-helix, our model indicates that the Lys301 of the 300-helix (Lys293–Lys301) of the SP domain also plays key role in interaction with the FVIIIa. The 301-helix interacts with both A2 and A3 domains. Over the simulation period, we observed stable ion-pair stabilization between the Lys301 of 300-helix and Glu683 of the A2 domain of FVIIIa. The A3-domain residues Glu1793 and Gln1796 also interact with the 300-helix of the SP domain.

The EGF2 domain of FIXa makes extensive interactions with the three β-sheets (Gln1692–His1697, Asn1770–Met1772 and Thr1814–Lys1818) of the A3 domain. The EGF2 domain region surrounding Asn91 residue and the 1811–1818 sequence of A3 domain were suggested to be involved in FVIIIa.FIXa interactions [17,22]. As shown in Table 1, the side-chain of Lys91 of EGF2 domain makes hydrogen-bonding interactions with the side-chains of Thr1695, Lys1693 and Asn1770. Similarly the EGF2 domain residues Thr87, Asn89, Arg94, Asn101 and Asp104 make

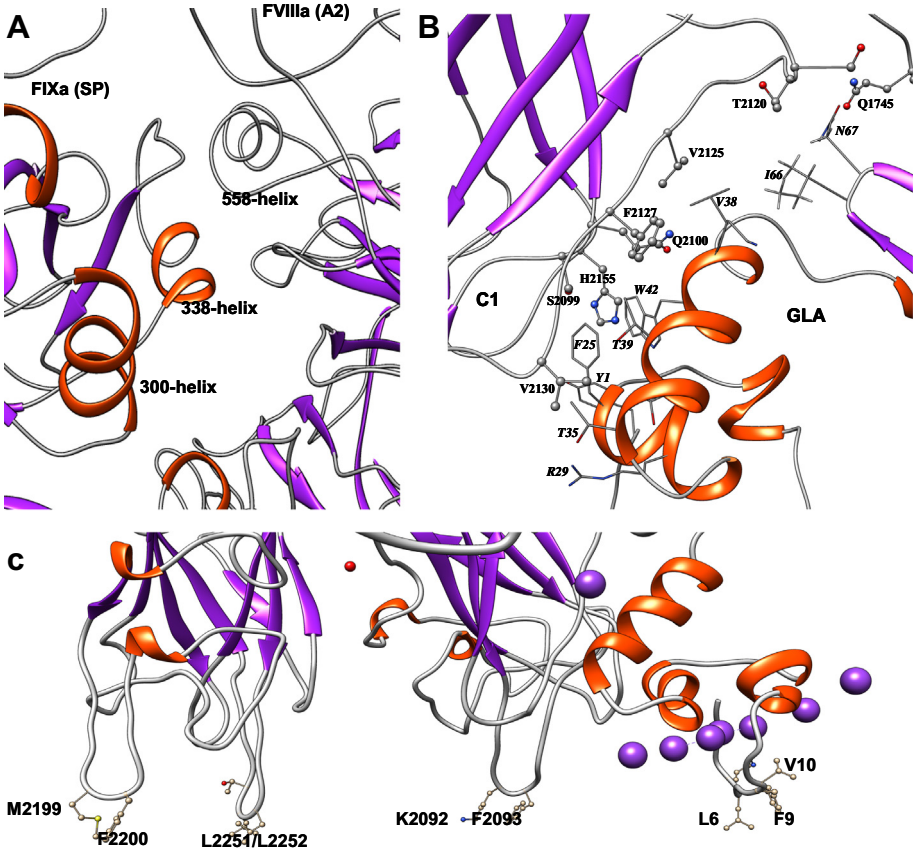

Fig. 4. Residues involved in interactions (A) between EGF2-SP domains of FIXa and A2 domain of FVIIIa; (B) between GLA-EGF1 domains of FIXa and A3–C1 domains of FVIIIa. (C) the alignment of the membrane-binding residues in the four hydrophobic spikes of C1–C2 domains and the GLA domain of FIXa within the tenase complex.

extensive polar interactions with the three β-sheets of the A3 domain.

It is also worth noting that the predicted orientation of the 338-helix binding with the A2-domain surface within the tenase complex is encouragingly similar to the corresponding orientation in structurally and functionally homologous prothrobinase (FVa:FXa) complex. In a recent X-ray crystal structure of the partially resolved complex from venom *Pseudonaja textilis*, the SP domain of FXa was observed to bind to the A2 domain of FVa in the same cleft-region of A2–A3 interface of FVa [23]. Given that there is remarkable similarity of binding orientation between our model of tenase complex and the prothrombinase complex provides a reasonable ground of credence to the validity of our model.

3.6. A3–C1 domain interactions with GLA-EGF1 domains

The light-chain domains A3 and C1 of FVIIIa interact with the GLA and EGF1 domains of FIXa. From the modeling perspective, it is unlikely that the C2-domain interacts with FIXa during the complex formation. The domain-domain interactions are predominantly hydrophobic with relatively less polar interactions. As shown in Fig. 4B, the C1-domain loop (Asn2118–Ser2113) is the primary recognition motif for binding to the GLA-EGF1 domains of FIXa. The hydrophobic helical stack, spanning the residues Asn34–Asp47, connecting the GLA and EGF1 domains makes extensive interactions with C1 domain. The equilibrated structure shows that most of the loop residues of the sequence Asn2219–Ser2113 are within van der Waals' contact region of the GLA-EGF1 domain residues. Analysis of the hemophilia-A mutational database shows that a majority of the residues in the C1-loop region appear to cause mild to severe bleeding disorders in hemophilia patients. While some of these loop residues are directly involved in GLA domain interactions, mutation of other residues are most likely responsible for conformational changes in the loop structure that might in turn affect the productive binding of the GLA domain.

The C1–C2 domain region of FVIIIa has been well-characterized as the membrane interactive region in the intrinsic coagulation pathway. The X-ray crystal structure showed that the platelet binding region of C1 and C2 domains are characterized with four hydrophobic spikes that have been hypothesized to be the membrane insertion regions. Several site-specific mutagenesis studies have implicated that the specific hydrophobic and/or cationic residues at the four spikes altered the membrane binding affinity of FVIIIa protein [24,25]. The mutations of the residues Lys2092/Phe2093 of the C1 domain and Met2199/Phe2200/Leu2251/Leu2252 residues of the C2 domain have been shown to reduce the binding affinity of FVIIIa co-factor on the PL surface, suggesting that these residues might be responsible for membrane interactions [25]. While a similar data is not available for the role of specific residues of GLA domain involvement in membrane interactions, it has been shown that the GLA domain interacts with FVIIIa light-chain during the tenase complex formation [26]. Our current model shows that the ω-loop region of the GLA domain is at nearly the same plane of the hydrophobic spikes of the C1–C2 interface. As shown in Fig. 4C, our model shows that the residues Met2199/Phe2200/Leu2251/Leu2252 of the C2 domain, Leu2092/Phe2093 of the C1 domain and Leu6/Phe9/Val10 of the GLA domain align optimally at the same-level.

4. Concluding remarks

The recombinant FVIIIa and FIXa clotting factors that have been currently used for treating Hemophilia patients have very short shelf-life of less than 24 h. The inherent instability of the proteins is due to weak non-covalent domain–domain interactions. Guided by the existing experimental and genetic mutational data, we developed a consensus structural model for FVIIIa.FIXa complex. The knowledge of the potential protein–protein interaction sites between the cofactor and enzyme, obtained in the current study, could provide a useful direction towards identifying the "mutational hotspots" for experimental design of new synthetic variants.

Acknowledgments

This work was partly supported by the National Institutes of Health Grant (R15-HL082632). The computing resources were acquired by MRI grant from National Science Foundation (NSF-ACI-1126543). The atomic coordinates for the tenase complex may be obtained from the author upon request.

Appendix A. Supplementary data

Supplementary data associated with this article can be found, in the online version, at http://dx.doi.org/10.1016/j.bbrc.2014.08.078.

References

[1] E.W. Davie, K. Fujikawa, W. Kisiel, The coagulation cascade – initiation, maintenance, and regulation, Biochemistry 30 (1991) 10363–10370.
[2] K.G. Mann, M.E. Nesheim, W.R. Church, P. Haley, S. Krishnaswamy, Surface-dependent reactions of the vitamin K-dependent enzyme complexes, Blood 76 (1990) 1–16.
[3] H. Brandstetter, M. Bauer, R. Huber, P. Lollar, W. Bode, X-ray structure of clotting factor IXa – active-site and module structure related to Xase activity and hemophilia-B, Proc. Natl. Acad. Sci. U.S.A. 92 (1995) 9796–9800.
[4] A.R. Thompson, Structure, function, and molecular defects of factor-IX, Blood 67 (1986) 565–572.
[5] S.P. Leytus, D.C. Foster, K. Kurachi, E.W. Davie, Gene for human factor-X – a blood-coagulation factor whose gene organization is essentially identical with that of factor-IX and protein-C, Biochemistry 25 (1986) 5098–5102.
[6] I. Jagannathan, H.T. Ichikawa, T. Kruger, P.J. Fay, Identification of residues in the 558-loop of factor VIIIa A2 subunit that interact with factor IXa, J. Biol. Chem. 284 (2009) 32248–32255.
[7] S.P. Bajaj, A.E. Schmidt, A. Mathur, K. Padmanabhan, D.G. Zhong, M. Mastri, P.J. Fay, Factor IXa:factor VIIIA interaction-helix 330–338 of factor IX interacts with residues 558–565 and spatially adjacent regions of the A2 subunit of factor VIIIa, J. Biol. Chem. 276 (2001) 16302–16309.
[8] D. Venkateswarlu, Structural investigation of zymogenic and activated forms of human blood coagulation factor VIII: a computational molecular dynamics study, BMC Struct. Biol. 10 (2010) 7.
[9] J.A. Huntington, D.J.D. Johnson, 3KCG: Crystal structure of the antithrombin-factor IXa-pentasaccharide complex, Protein Data Bank, 2010.
[10] Y. Shikamoto, T. Morita, Z. Fujimoto, H. Mizuno, Crystal structure of Mg2+- and Ca2+-bound GLA domain of factor IX complexed with binding protein, J. Biol. Chem. 278 (2003) 24090–24094.
[11] H. Brandstetter, M. Bauer, R. Huber, P. Lollar, W. Bode, 1PFX: porcine factor IXA, Protein Data Bank, 1996.
[12] E.F. Pettersen, T.D. Goddard, C.C. Huang, G.S. Couch, D.M. Greenblatt, E.C. Meng, T.E. Ferrin, UCSF chimera – a visualization system for exploratory research and analysis, J. Comput. Chem. 25 (2004) 1605–1612.
[13] J.C.K. Ngo, M. Huang, D.A. Roth, B.C. Furie, B. Furie, Crystal structure of human factor VIII: implications for the formation of the factor IXa–factor VIIIa complex, Structure 16 (2008) 597–606.
[14] S.H. Qureshi, L.K. Yang, A.R. Rezaie, Contribution of the NH2-terminal EGF-domain of factor IXa to the specificity of intrinsic tenase, Thromb. Haemost. 108 (2012) 1154–1164.
[15] E.S.C. Shih, M.J. Hwang, A critical assessment of information-guided protein-protein docking predictions, Mol. Cell. Proteomics 12 (2013) 679–686.
[16] R. Mendez, R. Leplae, L. De Maria, S.J. Wodak, Assessment of blind predictions of protein–protein interactions: current status of docking methods, Proteins Struct. Funct. Bioinf. 52 (2003) 51–67.
[17] E. Bloem, H. Meems, M. van den Biggelaar, K. Mertens, A.B. Meijer, A3 domain region 1803–1818 contributes to the stability of activated factor VIII and includes a binding site for activated factor IX, J. Biol. Chem. 288 (2013) 26105–26111.
[18] A. Mathus, S.P. Bajaj, Protease and EGF1 domains of factor IXa play distinct roles in binding to factor VIIIa – importance of helix 330 (helix 162 in chymotrypsin) of protease domain of factor IXa in its interaction with factor VIIIa, J. Biol. Chem. 274 (1999) 18477–18486.
[19] M.D. Blostein, B.C. Furie, I. Rajotte, B. Furie, The GLA domain of factor IXa binds to factor VIIIa in the tenase complex, J. Biol. Chem. 278 (2003) 31297–31302.

[20] P.E. Bock, Active-site selective labeling of serine proteases with spectroscopic probes using thioester peptide chloromethyl ketones – demonstration of thrombin labeling using N-alpha-(acetylthio)acetyl-D-phe-pro-Arg-Ch2Cl, Biochemistry 27 (1988) 6633–6639.
[21] S. Hubbard, NACCESS: program for calculating accessibilities, 1992.
[22] P.H.N. Celie, P.J. Lenting, K. Mertens, Hydrophobic contact between the two epidermal growth factor-like domains of blood coagulation factor IX contributes to enzymatic activity, J. Biol. Chem. 275 (2000) 229–234.
[23] B.C. Lechtenberg, T.A. Murray-Rust, D.J.D. Johnson, T.E. Adams, S. Krishnaswamy, R.M. Camire, J.A. Huntington, Crystal structure of the prothrombinase complex from the venom of *Pseudonaja textilis*, Blood 122 (2013) 2777–2783.
[24] E.J. Husten, C.T. Esmon, A.E. Johnson, The active-site of blood-coagulation factor-Xa – its distance from the phospholipid surface and its conformational sensitivity to components of the prothrombinase complex, J. Biol. Chem. 262 (1987) 12953–12961.
[25] S.W. Lin, K.J. Smith, D. Welsch, D.W. Stafford, Expression and characterization of human factor-IX and factor-IX–factor-X chimeras in mouse C127 cells, J. Biol. Chem. 265 (1990) 144–150.
[26] C. Manithody, L. Yang, A.R. Rezaie, Identification of a basic region on tissue factor that interacts with the first epidermal growth factor-like domain of factor X, Biochemistry 46 (2007) 3193–3199.